Received July 13, 2020, accepted July 22, 2020, date of publication July 29, 2020, date of current version August 12, 2020.

Digital Object Identifier 10.1109/ACCESS.2020.3012723

Matrix-Partitioned DDM for the Accurate Analysis of Challenging Scattering Problems

YING-YU LIU, MING-DA ZHU, (Member, IEEE), CHANG ZHAI, PENG HOU, AND YU ZHANG

Shaanxi Key Laboratory of Large Scale Electromagnetic Computing, Xidian University, Xi'an 710071, China

Corresponding author: Yu Zhang (yuzhang@mail.xidian.edu.cn)

ABSTRACT A matrix-partitioned domain decomposition method based on integral equation using the out-of-core iterative solver is presented for accurately analyzing challenging electromagnetic scattering problems with limited memory. The proposed method is based on the domain decomposition strategy, which decomposes the original large complex matrix of the electrically large problem into several sub-matrices of the electrically small sub-problems. Then, the out-of-core solver is used to solve the partitioned matrix equation panel by panel. In the process of constructing sub-problems, the proposed method does not introduce any additional unknowns. Thus, it can significantly reduce memory consumption, expanding the scale of the problem that can be solved. Numerical examples demonstrate that the method is very accurate even for the EM scattering targets the RCS of which are below −40 dBsm. And it can completely eliminate the pseudo edge effect which often occurs in the implementation of the domain decomposition method. In addition, modeling and partitioning the subdomains of the proposed method is easy and flexible.

INDEX TERMS Matrix partitioning, domain decomposition, surface integral equations, out-of-core solver.

I. INTRODUCTION

Accurate and efficient numerical analysis of large-scale electromagnetic (EM) systems [1]–[6] is always a hot research topic in computational electromagnetics. With the increasing requirements of the accuracy, efficiency, and simulation scale of electrically large targets and complex structures, there are new challenges to the simulation capability of modern computational electromagnetics. In particular, the rapid increase in electrical scale has led to a sharp increase in the computational requirements for full-wave EM field simulation. The surface integral equation (SIE) of method of moment (MoM) is a very powerful tool for the solution of EM radiation and scattering problems [7]–[11]. MoM [12], [13] combined with Rao–Wilton–Glisson (RWG) functions [14] is one of the most classic frequency-domain numerical approach. The SIE only needs to perform geometric mesh on the boundary surface. As SIE automatically satisfies the boundary conditions of the radiation, there is no need to set the additional truncation boundary. Moreover, SIE does not suffer from the numerical dispersion error. Hence, SIE has the advantage of high computation accuracy.

The associate editor coordinating the review of this manuscript and approving it for publication was Wen-Sheng Zhao.

The traditional MoM can hardly be applied into the analysis of electrically large problems because of the limitation on the memory. The high computational complexity resulting from the dense MoM matrix, has been overcome by the fast integral solvers. The first category of fast integral solvers is an algorithm based on the fast Fourier transform [15]–[17], such as the adaptive integration method, etc. The second category is the algorithms based on low rank matrix compression [18]–[21]. Typical methods of the third category based on the series expansion of the integral kernel [22]–[26] include fast multipole method and its extension: multilevel fast multipole algorithm (MLFMA). Theoretically, they accelerate the calculation of matrix-vector multiplication which is essential to an iterative process. The computational complexity can be decreased from $O(N^2)$ to $O(N\log N)$, which greatly improves the computational efficiency. However, even for MLFMA [24]–[26], it is difficult to deal with EM problems of thousands of wavelengths with limited computing resources. Another strategy to improve the computing capability of MoM is the parallel solver based on clusters. However, for some electrically large objects of real-world problems which require a huge amount of memory for computing, it is quite difficult to be solved on the existing distributed memory clusters. The out-of-core solver can break

the limitation of the clusters' memory, and it can be effectively implemented without reducing the accuracy. Therefore, in order to furtherly expand the scale of the problem to be solved, the parallel solver is combined with the out-of-core solver in this work. [27].

In order to break the bottlenecks of SIE, we combine two approaches in this article, namely the out-of-core solver and the domain decomposition strategy [28]–[42]. These two approaches are essentially based on the idea of ''dividing and conquering''. On one hand, the out-of-core solver refers to partitioning an original large matrix into several small sub-matrices which transfers the huge memory pressure for solving the matrix equation of MoM. On the other hand, the domain decomposition strategy refers to partitioning an original problem into several small sub-problems with small memory requirements and easy to solved. In recent years, the domain decomposition method based on the surface integral equations (SIE-based DDM) has attracted much attention, which is a feasible and efficient method for solving complex and large problems. Generally, the SIE-based DDMs can be categorized into two types: The enclosed-DDM (E-DDM) [28]–[33] is to partition the whole solution domain into many subdomains, and each subdomain is enclosed by a closed surface. The other type does not require the subdomain to be enclosed by a closed surface, which is referred to as unclosed-DDM (U-DDM) [34]–[42]. The U-DDM method consists of the overlapping domain decomposition method (ODDM) [34]–[37] containing a buffer, and non-overlapping domain decomposition method (NDDM) [38]–[42] without a buffer.

On one hand, since E-DDM introduces a manual interface to construct a closed surface, it cannot be used to simulate an open-structure target, and it causes great inconvenience to modeling. This brings great limitation to this type of domain decomposition. On the other hand, some U-DDM methods need additional unknowns, and the current across the boundaries is not completely continuous. The increased unknowns impose a heavy burden on the requirement of memory and computation, especially when the EM problem is large with a lot of subdomains. In this work, we investigate a novel matrix-partitioned domain decomposition method based on out-of-core solver (out-of-core MP-DDM), aiming to address accurate analysis of electrically large targets in engineering applications. During the out-of-core computation, only a portion of the matrix is transferred from the hard disk to the random access memory (RAM) which participates in the computation at a certain period. The entire computation is done by the data exchange between the internal and external memory. Moreover, the proposed scheme does not require modifications on the original CAD object, nor does it introduce artificial interfaces and auxiliary unknowns. There is no need to construct an additional contour domain or overlapping regions for the adjacent subdomains. This method uses the full RWG basis functions across the boundaries, which guarantee the continuity of current across the subdomains. Thus, no additional transmission

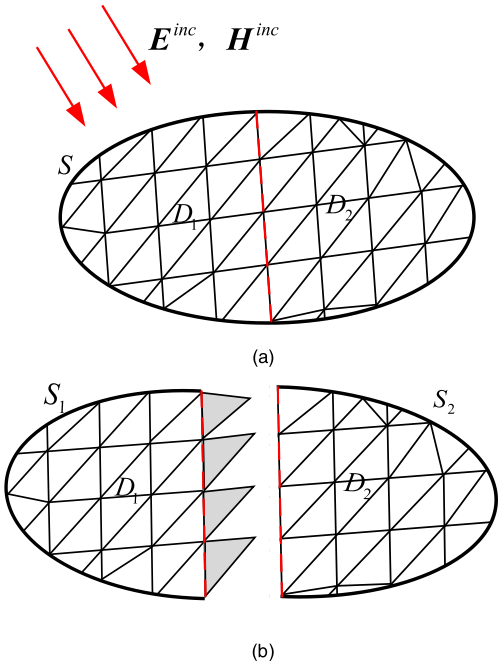

FIGURE 1. Schematic diagram of out-of-core MP-DDM: (a) the original closed surface; (b) the opened decomposition surface.

conditions need to be implemented on the boundaries of the subdomains. The matrix-partitioned method proposed in this article, is a domain decomposition scheme which does not introduce additional unknowns compared to the overall solution. During the calculation process, the dimension of the system matrix can be kept constant, and the submatrix of each subdomain is independently evaluated. The domain decomposition method in this article is a preconditioner of the SIE method, and it is implemented in a matrix-partitioned manner during the calculation process.

This article is organized as follows. In Section II, the two strategies of domain decomposition method and out-of-core solver are proposed, and the singular integrals are described in detail. In Section III, several numerical examples are demonstrated, which verify the accuracy and efficiency of the proposed method. Moreover, the simulation of a thousand-wavelength ship highlights the computing power of the method. Conclusion are given in Section IV.

II. THEORY

A. DOMAIN DECOMPOSITION STRATEGY

It is assumed that there is a 3-D PEC object in the free space, where $(\boldsymbol{E}^{inc}, \boldsymbol{H}^{inc})$ is the incident field. D is the domain of the arbitrary shaped scattered object, S denotes the surface of D, as shown in Fig. 1(a). From the equivalent principle and the boundary conditions of the EM field, the surface integral equations (SIEs) can be established on S. Therefore, the unknown surface currents $\boldsymbol{J}_s$ are expanded with the RWG basis functions (RWGs) as follows

$$\boldsymbol{J}_S = \sum_{n=1}^{N} I_n^S \boldsymbol{f}_n^S(\boldsymbol{r}'), \tag{1}$$

where N is the unknown number, I_n is the unknown coefficient, and $\boldsymbol{f}_n^S(\boldsymbol{r}')$ is the RWGs. In order to solve the SIEs, the MoM is employed. For the original problem, the matrix equation of MoM can be written as

$$[\boldsymbol{Z}][\boldsymbol{I}] = [\boldsymbol{V}], \tag{2}$$

where the elements of the above equation can be evaluated as

$$Z_{mn} = jk\eta \int_{T_m^+ + T_m^-} \boldsymbol{f}_m^S(\boldsymbol{r}) \cdot \int_{T_n^+ + T_n^-} \left[\boldsymbol{f}_n^S(\boldsymbol{r}') + \frac{1}{k^2} \nabla' \bullet \boldsymbol{f}_n^S(\boldsymbol{r}') \nabla \right] G(R)\, ds' ds, \tag{3}$$

$$V_m = \int_{T_m^+ + T_m^-} \boldsymbol{f}_m^S(\boldsymbol{r}) \bullet \boldsymbol{E}^{inc} ds, \tag{4}$$

where $\eta = \sqrt{\mu/\varepsilon}$, $k = \omega\sqrt{\mu\varepsilon}$, and $G(R) = e^{-jkR}/(4\pi R)$ are the wave impedance, the wave number, and the Green's function in the free space, respectively. $R = |\boldsymbol{r} - \boldsymbol{r}'|$ represents the distance from the source point to the field point, $\boldsymbol{f}_m^S(\boldsymbol{r})$ is the testing function, using the Galerkin testing method.

Decompose domain D into two domains D_1 and D_2, thus S is decomposed into two open sub-surfaces S_1 and S_2. The red dotted line in the figure indicates the boundary at which the subdomains are separated. In order to ensure the completeness of the RWGs, it is necessary to supplement the other triangle of the triangle pair at the boundary line, as shown in the shaded part of Fig. 1(b). This operation does not require any actual modifications to the computer-aided design (CAD) model, as all triangle information is already given in the original meshing grid. We only need to do some reuse of the information of the shadow triangles. It is worth noting that the reuse of the grid information does not introduce any new unknowns. If there are N RWGs $\boldsymbol{f}_n^S(\boldsymbol{r})$ on the surface S, N_1 RWGs on S_1, and N_2 RWGs on S_2, respectively, the current expansion is written as

$$\boldsymbol{J}_S = \sum_{n=1}^{N} I_n^S \boldsymbol{f}_n^S(\boldsymbol{r}) = \sum_{n=1}^{N_1} I_{1,n}^{S_1} \boldsymbol{f}_{1,n}^{S_1}(\boldsymbol{r}) + \sum_{n=1}^{N_2} I_{2,n}^{S_2} \boldsymbol{f}_{2,n}^{S_2}(\boldsymbol{r}). \tag{5}$$

The total number of basis functions of each subdomain equals the number of basis functions of the original model, which is $N_1 + N_2 = N$. As it is necessary to complete the triangle pairs at the dividing lines of the subdomains, the triangle pairs only need to be supplement in just one of the subdomains. For the system problem of subdomains shown in Fig. 1(b), the system of equations can be written as

$$\begin{bmatrix} \boldsymbol{Z}_{11} & \boldsymbol{Z}_{12} \\ \boldsymbol{Z}_{21} & \boldsymbol{Z}_{22} \end{bmatrix} \begin{bmatrix} \boldsymbol{I}_1 \\ \boldsymbol{I}_2 \end{bmatrix} = \begin{bmatrix} \boldsymbol{V}_1 \\ \boldsymbol{V}_2 \end{bmatrix}, \tag{6}$$

where the matrices Z_{11} and Z_{22} describe self-actions on the two subdomains D_1 and D_2, respectively. Z_{12} and Z_{21} the interactions between different subdomains. As the sum of the unknowns of S_1 and S_2 remains the same as the number of unknowns in the original problem S, the dimensions of the matrices of (2) and (6) are unchanged.

Rewrite matrix equation (6) in the form of a linear system of equations,

$$\begin{cases} \boldsymbol{Z}_{11}\boldsymbol{I}_1 + \boldsymbol{Z}_{12}\boldsymbol{I}_2 = \boldsymbol{V}_1 \\ \boldsymbol{Z}_{21}\boldsymbol{I}_1 + \boldsymbol{Z}_{22}\boldsymbol{I}_2 = \boldsymbol{V}_2. \end{cases} \tag{7}$$

When the matrix vector multiplication (MVM) is calculated along the row, a panel of the matrix is calculated in core. The panel of the MVM is also decomposed into two portions $\boldsymbol{Z}_{ii}\boldsymbol{I}_i$ and $\boldsymbol{Z}_{ij}\boldsymbol{I}_i$, and the number of rows in each panel is equal to the number of unknowns in the subdomain. Denote the interaction $\boldsymbol{Z}_{ij}\boldsymbol{I}_i$ between subdomains as $\Delta\boldsymbol{V}_i(\boldsymbol{Z}_{ij})$. The strategy of correcting $\Delta\boldsymbol{V}_i(\boldsymbol{Z}_{ij})$ using mutual impedance is referred as to the DDMZ. If subdomains of equal size are assumed, when the whole domain is decomposed into n subdomains, the storage complexity of the method is $O\left((N/n)^2\right)$, and the complexity of the MVM is still $O\left(N^2\right)$ per iteration. To reduce the computational complexity of MVM, the linear equations (7) can be modified as follows,

$$\begin{cases} \boldsymbol{Z}_{11}\boldsymbol{I}_1 + \langle \boldsymbol{f}_1(\boldsymbol{r}), -\eta L\left(\boldsymbol{f}_2(\boldsymbol{r}')\right)\rangle \boldsymbol{I}_2 = \boldsymbol{V}_1 \\ \langle \boldsymbol{f}_2(\boldsymbol{r}), -\eta L\left(\boldsymbol{f}_1(\boldsymbol{r}')\right)\rangle \boldsymbol{I}_1 + \boldsymbol{Z}_{22}\boldsymbol{I}_2 = \boldsymbol{V}_2, \end{cases} \tag{8}$$

$$L(\boldsymbol{X}) = -jk \int_S \left[\boldsymbol{X}(\boldsymbol{r}') + \frac{1}{k^2}(\nabla' \cdot \boldsymbol{X}(\boldsymbol{r}'))\nabla \right] G(R) ds'. \tag{9}$$

According to the auxiliary bit function theory, we have

$$\begin{cases} \boldsymbol{Z}_{11}\boldsymbol{I}_1 - \langle \boldsymbol{f}_1(\boldsymbol{r}), \boldsymbol{E}_{12}\rangle = \boldsymbol{V}_1 \\ -\langle \boldsymbol{f}_2(\boldsymbol{r}), \boldsymbol{E}_{21}\rangle + \boldsymbol{Z}_{22}\boldsymbol{I}_2 = \boldsymbol{V}_2. \end{cases} \tag{10}$$

We arrive at the following expression as given by

$$\begin{cases} \boldsymbol{Z}_{11}\boldsymbol{I}_1 = \boldsymbol{V}_1 + \Delta\boldsymbol{V}_1(\boldsymbol{E}_{12}) \\ \boldsymbol{Z}_{22}\boldsymbol{I}_2 = \boldsymbol{V}_2 + \Delta\boldsymbol{V}_2(\boldsymbol{E}_{21}). \end{cases} \tag{11}$$

In MVM process, the multiplication of $\boldsymbol{Z}_{ij}$ and $\boldsymbol{I}_j$ for obtaining the coupling voltage between subdomains, can be equivalent to the process of calculating the near field of the subdomain D_i generated by the surface current $\boldsymbol{I}_j^{(k+1)}$ on the subdomain D_j, and getting the inner product of the obtained near field and weight functions to obtain the coupling voltage ($\Delta\boldsymbol{V}_i(\boldsymbol{E}_{ij})$) between subdomains. With this scheme, we can eliminate the need to calculate and store the mutual impedance matrix in (6), and only calculating the additional field excitation in each iteration. The coupling voltage ($\Delta\boldsymbol{V}_i(\boldsymbol{E}_{ij})$) can be obtained using the near scattered field generated by the surface currents from other subdomains That can furtherly reduce the storage complexity. The strategy of correcting $\Delta\boldsymbol{V}_i(\boldsymbol{E}_{ij})$ using only the near field is denoted as the DDME.

B. CALCULATION OF SINGULAR INTEGRALS

In the last sub-section we mentioned that using the coupling voltage ($\Delta\boldsymbol{V}_i(\boldsymbol{E}_{ij})$) to correct $\boldsymbol{V}$ can effectively reduce the storage complexity, for the shaded triangles in Fig. 1(b), that is, the part where the two subdomains reusing, there is a near-field singularity of $\Delta\boldsymbol{V}_i(\boldsymbol{E}_{ij})$.

$$\boldsymbol{E}_S(\boldsymbol{J}) = \eta L(\boldsymbol{J}) = -jk\eta \int_S \left[\boldsymbol{J}(\boldsymbol{r}') + \frac{1}{k^2}(\nabla' \cdot \boldsymbol{J}(\boldsymbol{r}'))\nabla \right] G(R) ds'. \tag{12}$$

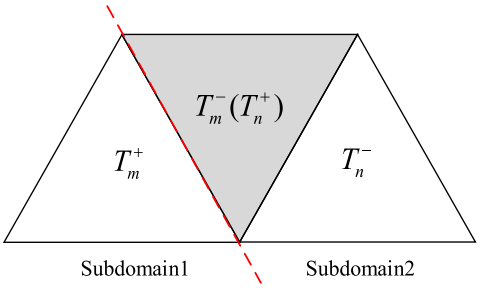

FIGURE 2. Schematic diagram of special impedance element.

The Green's function and its gradient results in the singular integrals when computing the surface EM field. For the shaded triangles in Fig. 1(b), which are shared between two adjacent subdomains to form the complete RWGs, there are singularities when computing the near field on these triangular patches. Accordingly, these triangular patches should be specially handled.

In order to eliminate the error caused by the singular points in the surface field computation, we do the correction by multiplying the impedance element by the current coefficient in the shaded triangles that shared by the adjacent subdomains, as follows

$$\Delta \boldsymbol{V}_i(\boldsymbol{E}_{ij}, \boldsymbol{Z}_{ij}^{1/4}) = \Delta \boldsymbol{V}_i(\boldsymbol{E}'_{ij}) - \Delta \boldsymbol{V}_i(\boldsymbol{Z}_{ij}^{1/4} \cdot \boldsymbol{I}_i^{1/4}), \quad (13)$$

where $\boldsymbol{E}'_{ij}$ is the near-field value at the sampling point of the triangular patches except for the shaded triangles. $\boldsymbol{Z}_{ij}^{1/4}$ denotes quarter of the impedance element value of the shaded triangles. $\boldsymbol{I}_i^{1/4}$ denotes the corresponding current coefficients of the RWGs on the triangle pairs formed by the shaded triangles and the triangles adjoining with them.

The complete impedance element Z_{mn} should consist of four parts, as given by

$$Z_{mn} = Z_{T_m^+ T_n^+} + Z_{T_m^+ T_n^-} + Z_{T_m^- T_n^+} + Z_{T_m^- T_n^-}. \quad (14)$$

In this approach, $\boldsymbol{Z}_{ij}^{1/4}$ is only related to the shaded triangles. For example, as shown in Fig. 2, the 1/4 impedance element $Z_{ij_{mn}}^{1/4}$ only consists of one part as follows

$$Z_{ij_{mn}}^{1/4} = Z_{T_m^- T_n^+}. \quad (15)$$

Then, the sparse impedance matrix (actually a vector) $\boldsymbol{Z}_{ij}^{1/4}$ should contain only m impedance elements. m is the number of the basis functions across the boundary lines. The matrix $\boldsymbol{Z}_{ij}^{1/4}$ is filled only once, which can be reused in each iteration. The strategy of correcting $\Delta \boldsymbol{V}_i(\boldsymbol{E}_{ij}, \boldsymbol{Z}_{ij}^{1/4})$ using the near field combined with the quarter impedance elements across the boundary lines is denoted as the DDMEZ. By this method, smaller computing resources are required to solve larger EM problems while ensuring the accuracy of computation.

C. OUT-OF-CORE ITERATIVE SOLVER

The MoM obtain a dense matrix equation, resulting in storage complexity $O\left(N^2\right)$. Since the memory capacity cannot meet the storage requirements involving large complex dense matrix problems, we develop an out-of-core iterative solver that some portions of the matrix are written to the hard disk. Hence, the large matrix generated by the original problem is decomposed into sub-matrices that can be addressed in RAM.

In the traditional implementation of MoM, the whole system matrix should be stored. However, one task of DDM is to reduce the demand for computer memory of integrated EM computation. Therefore, by combining the out-of-core solver, we calculate the impedance matrix and the voltage vector of the whole system in different subdomains. We fill these small sub-matrices in RAM in turn, and write them to the hard disk as soon as it is filled. Sub-matrices are read into RAM in turn when solving the whole system matrix equation panel-wisely. For the DDME strategy, there is no need to fill and store the mutual-impedance sub-matrices. For the DDMEZ strategy, the mutual-impedance sub-matrices that needs to be filled and stored is only a vector. This is an alternative way to apply DDM to large and complex EM problems.

In out-of-core MP-DDM, the generalized minimum residual method (GMRES) in Krylov subspace [43] is used to solve (6). The GMRES solver selects the relative residual error as the convergence criterion, and its termination criterion is defined as

$$\varepsilon = \frac{\left\| P^{-1}\left(Ax - b\right)\right\|_2}{\left\| P^{-1} b\right\|_2}. \quad (16)$$

For the convenience of description, (6) is rewritten as

$$\begin{bmatrix} \boldsymbol{A}_{11} & \boldsymbol{A}_{12} \\ \boldsymbol{A}_{21} & \boldsymbol{A}_{22} \end{bmatrix} \begin{bmatrix} \boldsymbol{X}_{k,1} \\ \boldsymbol{X}_{k,2} \end{bmatrix} = \begin{bmatrix} \boldsymbol{B}_1 \\ \boldsymbol{B}_2 \end{bmatrix}, \quad (17)$$

where k represents the number of iterations.

From the domain decomposition strategy in subsection A, we know that the unknowns among the subdomains are independent of each other. The mutual couplings between subdomains are effected by $\Delta \boldsymbol{V}_i$. Specific strategies include DDMZ ($\Delta \boldsymbol{V}_i(\boldsymbol{Z}_{ij})$), DDME ($\Delta \boldsymbol{V}_i(\boldsymbol{E}_{ij})$) and DDMEZ ($\Delta \boldsymbol{V}_i(\boldsymbol{E}_{ij}, \boldsymbol{Z}_{ij}^{1/4})$). Therefore, the unknown coefficients in the matrix equation of the system are sorted by subdomain. That is, the first panel row corresponds to the first subdomain, the second panel row corresponds to the second subdomain, and so on. Different from the way the global solution is solved, at each iteration, the initial N-dimension current coefficient vector is partitioned according to the number of subdomains and the number of unknowns of each subdomain. Each subdomain retains only the portion of the current coefficients of its own subdomain, thereby converting the global MVM into the subdomain's MVM, as shown in Fig. 3.

Taking two subdomains as an example, we partition the initial current coefficient vector first as follows

$$\boldsymbol{X}_0 = \begin{bmatrix} \boldsymbol{X}_{0,1} \\ \boldsymbol{X}_{0,2} \end{bmatrix}, \quad (18)$$

where,

$$\begin{aligned} \boldsymbol{X}_0 &= \left[x_{0,1} \ldots x_{0,N}\right] \\ \boldsymbol{X}_{0,1} &= \left[x_{0,1} \ldots x_{0,N_1}\right] \\ \boldsymbol{X}_{0,2} &= \left[x_{0,N_1+1} \ldots x_{0,N}\right]. \end{aligned} \quad (19)$$

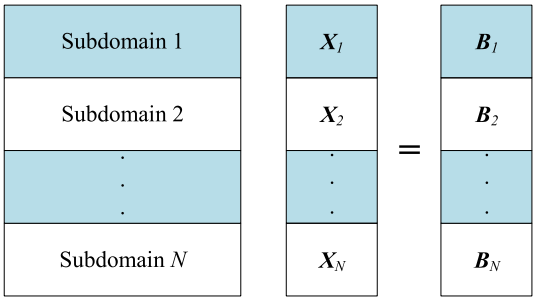

FIGURE 3. Schematic diagram of partitioning and assigning the global current coefficient vector.

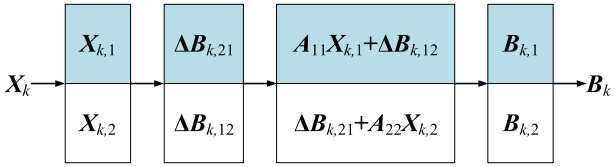

FIGURE 4. Schematic diagram of matrix vector multiplication in each step.

For the GMRES solver, in the MVM process of each iteration, the mutual coupling between subdomains is calculated first and written to the hard disk, as shown in Fig. 4. Then the total MVM of each subdomain are calculated one by one. When generalizing to P subdomains, the calculation of MVM process in each step of GMRES is shown in Fig. 5. When the MVM is calculated along the row direction, a panel of the matrix is calculated in core. The panel of the MVM is also decomposed into two portions $\boldsymbol{A}_{ii}\boldsymbol{X}_i$ and $\Delta\boldsymbol{V}_i$, and the number of rows in each panel is equal to the number of unknowns in the subdomain.

If subdomains of equal size are assumed, when the whole domain is decomposed into n subdomains, the storage complexity of the method is reduced to $O\left((N/n)^2\right)$. For the DDMZ strategy, the out-of-core computing programs contain a large number of operations on files. Because of the slow speed of accessing disk data, I/O performance obviously becomes an important limiting factor than CPU performance when dealing with large data problems. Although the large complex dense matrix $\boldsymbol{Z}$ is decomposed into small sub-matrices, the small complex matrices are still large for I/O operations, which cause a long I/O time. In contrast, the DDME and DDMEZ strategies can significantly reduce the I/O time and the computational complexity of MVM. We can further shorten the I/O time by changing the text input and output to binary input and output.

III. NUMERICAL RESULTS

In this section, we study the performance of the proposed out-of-core MP-DDM via numerical experiments. Firstly, through an open-structure model and a closed-structure model, the characteristics of the matrix elements of the system are studied. The proposed method proved to keep the total number of unknowns unchanged, while the well-conditioned DDM system matrix equation provides robust convergence in the numerical experiments. Secondly, through comparing with the analytical solution, the accuracy of out-of-core MP-DDM for the EM scattering problem is certificated. Thirdly, the surface current continuity of the low RCS carrier simulated by the proposed method is analyzed. The numerical result of the conventional single-domain SIE method (SD-SIE) is compared with it to prove the effective suppression of the proposed new transmission conditions on the reflected waves at the boundary between adjacent subdomains. Finally, an electrically large problem of practical interest is included to demonstrate the capability of the proposed method.

MVM Process in GMRES Solver

Start: Partition the initial current coefficient vector $\boldsymbol{X}_0$ into P current coefficient sub-vectors $\boldsymbol{X}_{0,i}$ of P subdomains

Step 1: For $i = 1, P$
- Input calculating information of subdomain i
- Input current coefficient sub-vector $\boldsymbol{X}_{0,i}$ of subdomain i
- For $j = 1, P$
  - If ($j \neq i$), then
    - Input calculating information of subdomain j
    - Calculate the interaction $\Delta\boldsymbol{B}_{ji}$ of subdomain i with subdomain j and write $\Delta\boldsymbol{B}_{ji}$ to the hard disk
  - End If
- End For

End For

Step 2: For $i = 1, P$
- Input calculating information of subdomain i
- Input current coefficient sub-vector $\boldsymbol{X}_{0,i}$ of subdomain i
- Calculate the self-action MVM $\boldsymbol{B}_i$ of subdomain i
- For $j = 1, P$
  - If ($j \neq i$), then
    - Input the interaction $\Delta\boldsymbol{B}_{ij}$ of subdomain j with subdomain i
    - Calculate the total MVM of subdomain i : $\boldsymbol{B}_i = \boldsymbol{B}_i + \Delta\boldsymbol{B}_{ij}$
  - End If
- End For

End For

Step 3: Combine the MVM of each subdomain by $\boldsymbol{B}_i$ to $\boldsymbol{B}$

The End

FIGURE 5. Calculation flow chart of matrix-vector multiplication in GMRES iterative solver.

For all numerical examples, the computations have been done on a workstation which consists of two six-core 64 bit Intel Xeon E5-2620 2.0 GHz CPUs, 64GB RAM and 6TB disk.

A. IMPEDANCE MATRIX ANALYSIS: A DIHEDRAL ANGLE AND A CUBE

Using $\boldsymbol{Z}_{ij}^{1/4}$ to correct $\Delta\boldsymbol{V}_i$, the near-field error due to the singularity can be significantly reduced, which improves the

computing accuracy. In order to verify the effectiveness of this strategy, we compute the equivalent impedance element value of each column by setting each element value in the current coefficient vector to 1 one by one. A typical dihedral angle model is chosen as the example, and the open surface is decomposed into two subdomains along two mutually perpendicular PEC faces, as shown in Fig. 6(a). The two subdomains are discretized with 5 and 3 unknowns, respectively. Since the basis functions of No. 3 and No. 5 in sub-domain 1 are two basis functions that cross the boundary line, we focus on the values of the impedance elements that contain these two basis functions. Since the simulation target is an open structure, the EFIE is chosen here for analyzing.

Fig. 6(b) and Fig. 6 (c) shows the comparison of impedance element value of out-of-core MP-DDM based on EFIE using DDMZ (black solid line), DDME (blue dashed line), and DDMEZ (red dashed line). This improvement can be observed very specifically by comparing the modulus values of the equivalent impedance elements. Theoretically, the impedance element produced by the DDMZ should be exactly the same as which produced by the global solution, except that the impedance element distribution is slightly different. It is obvious in Fig. 6 that the impedance element value with an error between the blue dashed line and the black solid line, that is the impedance element value containing the information of the basis function across the boundary line, is perfectly corrected in the red dashed line. Therefore, by using the boundary impedance to correct the deviation caused by the singularity of surface fields, the accuracy of the equivalent mutual impedance can be effectively improved.

Fig. 7 shows the eigenvalue distribution for the proposed DDM system matrix in (14). Cubes with a side length of 0.3 λ are decomposed into 2, 3, and 6 subdomains, and the EFIE is still used in this example. The corresponding eigenvalue spectra are demonstrated in Fig. 7 (a), (b) and (c), respectively. Although there are several eigenvalues distributed outside the shifted unit circle, most of the eigenvalues are clustered around a certain point, and they are well separated from the origin point. Thus, when using the Krylov iterative solver, it can converge quickly. Although the increase in the number of subdomains has some undesired influence on the eigenvalue spectra, the influence is not large. If the full basis functions across the boundary lines are considered as a transmission condition, the results indicate the validity of the proposed transmission condition. The reason is that the proposed DDM imposes current continuity across the boundary line by the full basis function between adjacent subdomains, which is an effective transmission condition on the subdomain boundaries. Moreover, such a strategy has no restrictions on the shape of the boundary line. This ensures the convenience of the domain decomposition when analyzing complex large-scale problems, and the subdomains can be adaptively constructed by the graph partitioning algorithms.

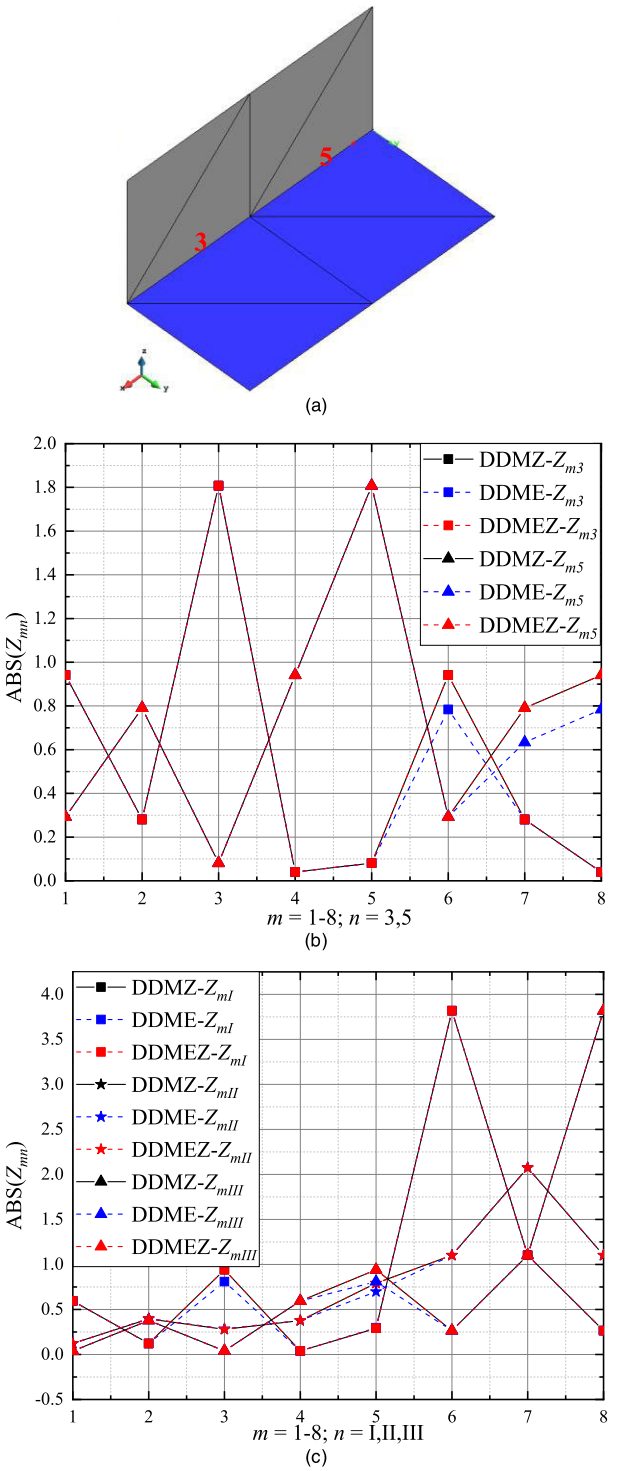

FIGURE 6. Comparison of impedance element value for an open PEC surface using out-of-core MP-DDM: (a) dihedral angle model; (b) impedance elements in columns 3 and 5 in subdomain 1; (c) 3 column impedance elements in subdomain 2.

B. ACCURACY STUDY: A PLANE-WAVE SCATTERING FROM A SPHERE

In this subsection, we examine the solution accuracy of the proposed method. We consider the EM scattering from a PEC sphere with radius 1.0 *m* at 1GHz, for which analytic solution

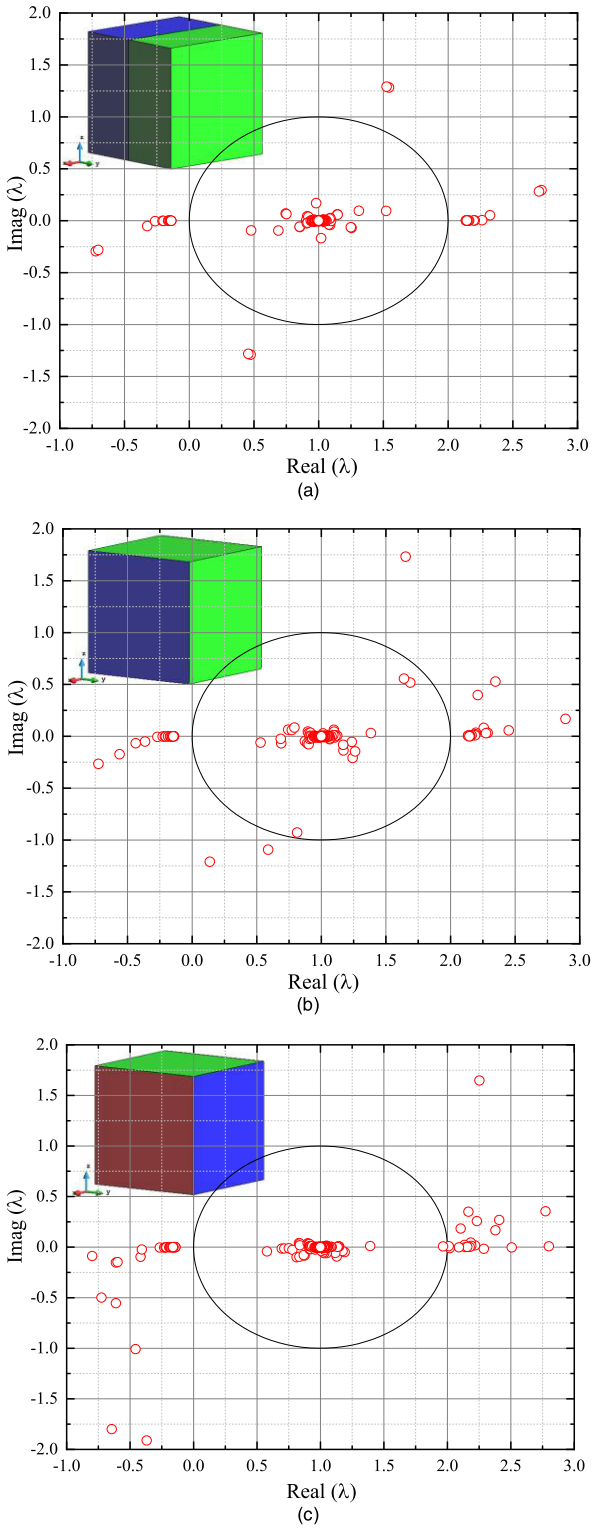

FIGURE 7. Eigen-spectrum for a PEC cube with respect to number of subdomains: (a) two subdomains; (b) three subdomains; (c) six subdomains.

is available in the form of Mie series. The sphere is decomposed into eight subdomains (calculated by DDMZ, DDME or DDMEZ), as shown in Fig. 8. The whole-domain solution by the SD-SIE (DDM1) is also presented as comparison.

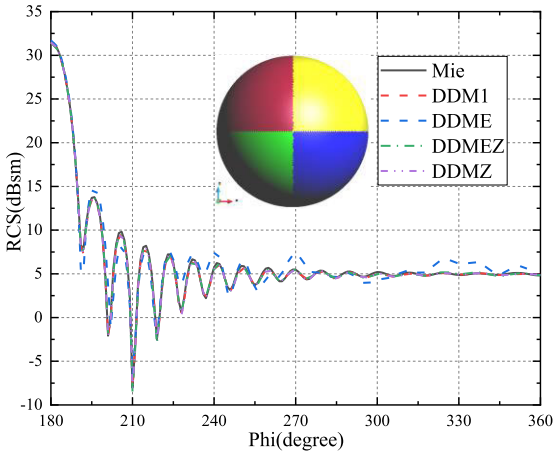

FIGURE 8. Bi-static RCS of a PEC sphere using analytic solutions, SD-SIE and out-of-core MP-DDM.

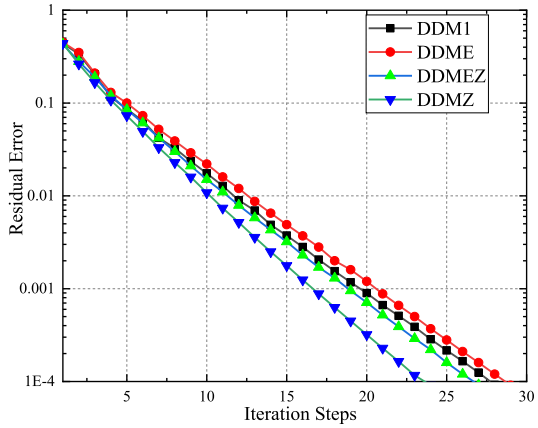

FIGURE 9. Iterative solver convergence of a PEC sphere using SD-SIE and out-of-core MP-DDM.

Then, we study the error convergence of the proposed method with respect to different strategies for calculating the interaction between subdomains. The convergence criterion is set to $\varepsilon = 1 \times 10^{-4}$. Fig. 9 shows the convergence of the SD-SIE (DDM1) and the MP-DDM using three different interaction calculating strategies (DDMZ, DDME or DDMEZ).

In Fig. 8, it is illustrated that the DDME strategy that uses only the near field to correct the $\Delta \boldsymbol{V}_i(\boldsymbol{E}_{ij})$, deviates from the analytical solution. The numerical results obtained from the out-of-core MP-DDM using DDMZ and DDMEZ strategies agree very well with the analytic solution. For the rate of convergence, DDME also has the worst performance. The DDMZ strategy has the fastest convergence rate, but its demand for hard disk storage resources is significantly higher than those of DDMEZ and DDME strategies. The convergence rate of DDMZ and DDMEZ are better than the whole-domain solution. Therefore, we use the proposed DDMEZ to form the MP-DDM strategy in the following examples.

The manner of impedance filling in each subdomain makes the structure of the block diagonal preconditioning more flexible in MP-DDM. We invert the self-action impedance matrix of each subdomain to form a stable preconditioner

TABLE 1. Computational statistics of a sphere.

Method	Unknowns	Storage	
		RAM	Hard Disk
SD-SIE	48582	35.17 GB	--
Out-of-core MP-DDM (DDMZ, DDME, DDMEZ)	6048 (Subdomain1) 6028 (Subdomain2) 6007 (Subdomain3) 5998 (Subdomain4) 6155 (Subdomain5) 6132 (Subdomain6) 6113 (Subdomain7) 6101 (Subdomain8)	4.40 GB	24.96 MB (*DDME*) 24.96 MB (*DDMEZ*) 30.77 GB (*DDMZ*)

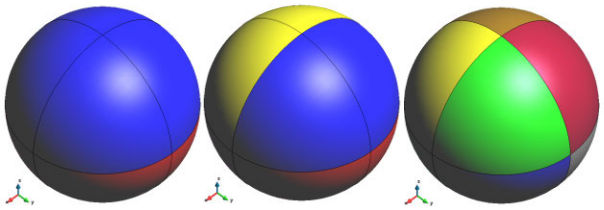

FIGURE 10. Sphere model and partitioning: (a) two subdomains; (b) four subdomains; (c) eight subdomains.

that is easy to implement. As shown in Table 1, the memory consumption of the proposed method is significantly reduced compared to SD-SIE. This breaks the storage bottleneck of the SIE method, making it possible to simulate the electrically large problem that could not be solved before.

Next, the CPU time and memory cost for a different number of subdomains are compared. The sphere is decomposed into 2, 4, and 8 subdomains respectively, as shown in Fig. 10. The sphere consisting of 2 subdomains is partitioned into 24499 and 24083 unknowns, respectively. The sphere consisting of 4 subdomains is partitioned into 12353, 12146, 12145, and 11938 unknowns, respectively. The results are shown in Fig. 11. And a comparison of computation time and memory consumption is given in Table 2. It can be seen that the advantages of this algorithm are obvious.

C. SURFACE CURRENT CONTINUITY: A PLANE-WAVE SCATTERING FROM A LOW RCS CARRIER

In this subsection, the scattering behavior of an almond is investigated using the out-of-core MP-DDM. The size of the almond is 0.97 m × 0.31 m × 0.04 m as shown in Fig. 12, which is partitioned into three subdomains along x direction with 588, 522, 204 unknowns, respectively. The plane-wave at 600MHz illuminates the PEC almond from $-x$ direction and the electric field is polarized in the $+z$ direction. The numerical results in Fig. 12 demonstrate the current continuity across the adjacent subdomains. The proposed method fully suppresses reflections from the boundary in a straightforward manner.

It is illustrated in Fig. 12 that the surface electric current distributions at 600MHz using the conventional SD-SIE method (DDM1) and the out-of-core MP-DDM (DDM3). The out-of-core MP-DDM gives a nearly identical solution to that of the SD-SIE method, and the erroneous reflections from

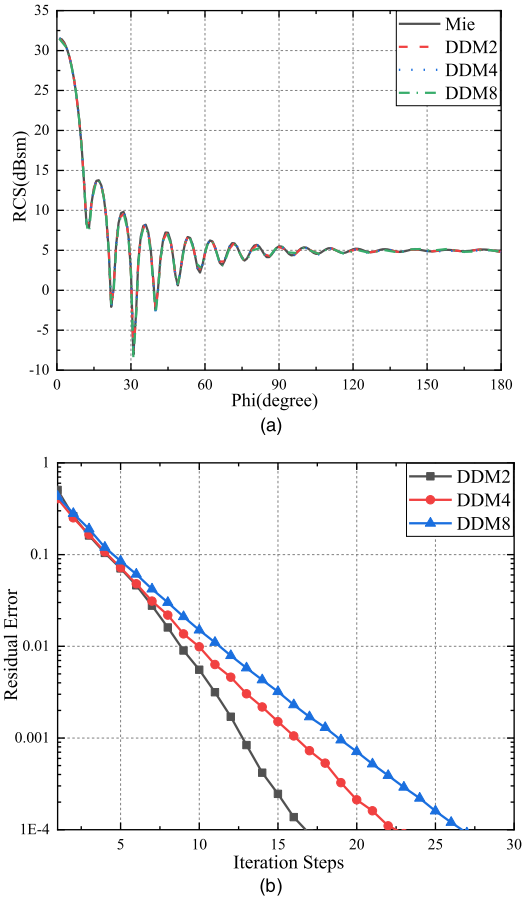

FIGURE 11. Bi-static RCS and iterative solver convergence of a PEC sphere with respect to number of subdomains: (a) bi-static RCS; (b) iterative solver convergence.

TABLE 2. Computational statistics of a sphere.

Method	Time	Storage	
		RAM	Hard Disk
SD-SIE	218.9s	35.17 GB	--
Out-of-core MP-DDM (DDM2, DDM4, DDM8)	268.8 s (*DDM2*) 274.5 s (*DDM4*) 312.4 s (*DDM8*)	17.59 GB (*DDM2*) 8.79 GB (*DDM4*) 4.40 GB (*DDM8*)	4.20 MB (*DDM2*) 11.12 MB (*DDM4*) 24.22 MB (*DDM8*)

the boundaries are suppressed completely, which demonstrate the current continuity across the adjacent subdomains. The bi-static RCS of the PEC almond using the four methods (including a commercial software (FEKO) and a traditional non-overlapping DDM (NDDM) [28]) are shown in Fig. 13 Evidently, the results obtained from FEKO, DDM1, and DDM3 agree very well even for the results below −40 dBsm. NDDM's results are unreliable below −30 dBsm. Fig. 14 shows the convergence of the SD-SIE method (DDM1) and the out-of-core MP-DDM (DDM3). The convergence criterion is set to $\varepsilon = 1 \times 10^{-3}$. The out-of-core MP-DDM can achieve convergence within 30 steps, while the SD-SIE method needs 52 steps.

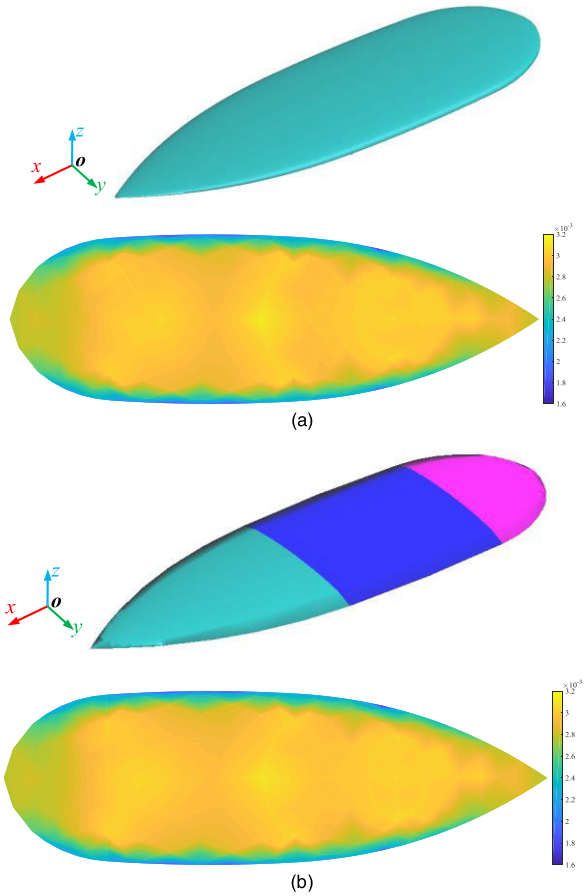

FIGURE 12. Domain partitions and surface current distributions (magnitude in A/m) on an almond: (a) DDM1; (b)DDM3.

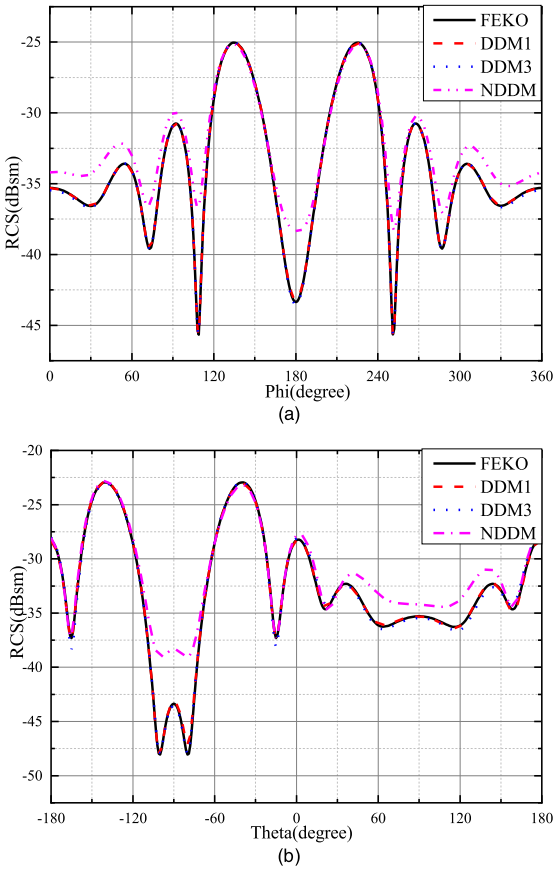

FIGURE 13. Bi-static RCS of an almond using MoM and out-of-core MP-DDM: (a) x-y plane; (b) x-z plane.

D. APPLICATION: A PLANE-WAVE SCATTERING FROM A SHIP

In this subsection, we s hall present a numerical example to demonstrate the capability of the proposed MP-DDM in simulating electrically large PEC targets. The out-of-core MD-DDM in the example is accelerated by MLFMA [51] to speed up the impedance filling of the subdomains and the MVM of iterative processes. By the octree structure formed by MLFMA in space, the unknowns can be adaptively grouped to realize the decomposition of subdomains, so that the proposed transmission conditions can be naturally introduced conveniently. The parallel scale is 12 processes. The convergence criterion is set to $\varepsilon = 5 \times 10^{-3}$.

The parameter of the ship is 160.57-m long, 24.10-m wide, and 29.76-m high, as shown in Fig. 15. The incident plane wave is toward the bow ($-x$), and the polarization direction is $+z$. The operating frequency is 2GHz. The whole ship model has 63,016,119 unknowns, which is decomposed into 76 subdomains by oct-tree graphical partitioning algorithm. The largest subdomain contains 1,879,869 unknowns. If the MLFMA global solution is used, at least 793.86 GB of memory would be required, while the peak memory of the domain decomposition solution is 17.48 GB. For the scattering problem of such an electrically large platform, the memory required for the global solution is too enormous for the

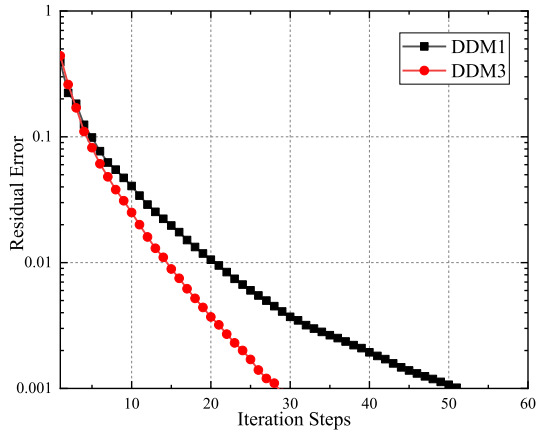

FIGURE 14. Iterative solver convergence of a PEC almond using SD-SIE and out-of-core MP-DDM.

workstation used in this study. With the domain decomposition method, the memory consumption is saved by approximately 97.7%. The surface current distribution is illustrated in Fig. 16, which shows a smooth current distribution without discontinuities on subdomain boundaries.

By the proposed method, a common workstation can analyze the EM problem of an electrically large target, which is a great convenience for the users. If the program is transplanted

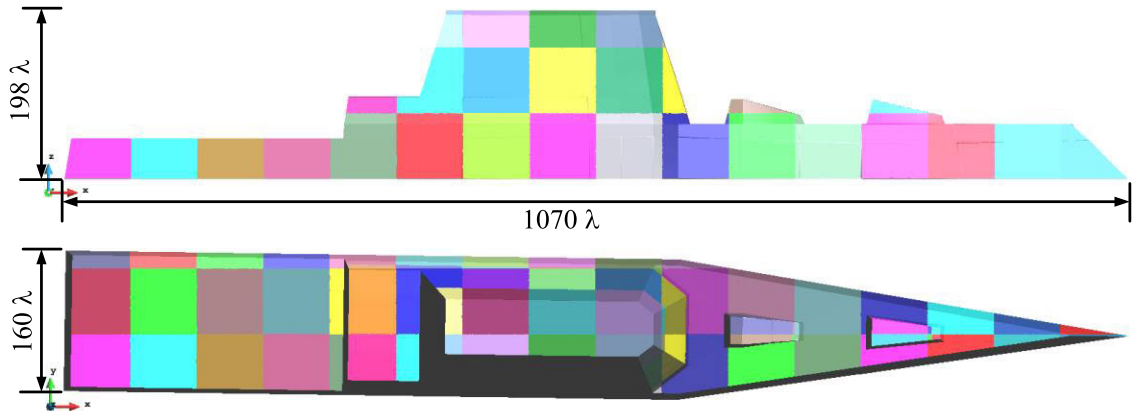

FIGURE 15. Ship model and partitioning.

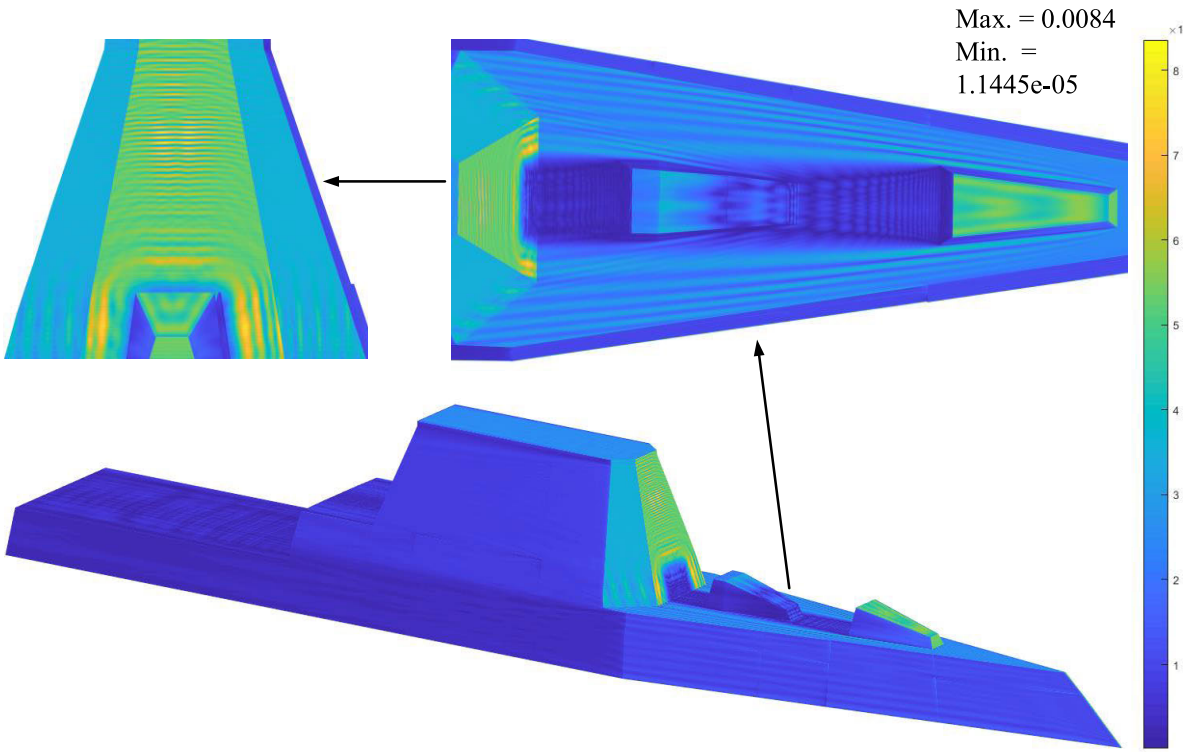

FIGURE 16. Surface current distributions (magnitude in A/m) on a ship.

to a high-performance computing platform, the scale of the problems that can be solved will double.

IV. CONCLUSION

A novel matrix-partitioned DDM based on SIE is proposed to solve challenging EM scattering from electrically large PEC objects with limited memory using an out-of-core solver. The surface continuity of the current is constrained by the full RWG basis functions in this article, which can effectively avoid unphysical reflections from the subdomain boundaries. This scheme of forcing the surface current continuity can also be regarded as a new transmission condition. There are three advantages of this scheme. The first is that there are no additional unknowns introducing, and the storage resources required for the computation are really small. The second one is to completely eliminate the reflected waves from the subdomain boundaries, and the proposed method is highly consistent with the results of the global solution. Third, the model can be arbitrarily decomposed, which simplifies the pre-processing operation and facilitates the analysis of large-scale multi-domain EM problems. The proposed MP-DDM method is effectively verified by several numerical examples involving open and closed objects. The results simulated by MP-DDM are in very good agreements with those obtained by single-domain SIE method, even for low RCS carriers. In addition, it has been shown that the

matrix eigenvalue spectrum of the DDM system performs well. Since the method can adaptively construct the load balancing subdomains through the mesher, the future work is to transplant the algorithm to the high performance computing platform for handling even larger objects with much more subdomains.

In the follow-up work, the half-RWG basis functions can be used for the non-conformal meshes at the boundary. However, it will cause the increase in the number of unknowns. By using the full-RWGs combing with half-RWGs can reduce the increase.

REFERENCES

[1] Y. Xu, H. Yang, R. Shen, L. Zhu, and X. Huang, "Scattering analysis of multiobject electromagnetic systems using stepwise method of moment," *IEEE Trans. Antennas Propag.*, vol. 67, no. 3, pp. 1740–1747, Mar. 2019.

[2] T. Su, L. Du, and R. Chen, "Electromagnetic scattering for multiple PEC bodies of revolution using equivalence principle algorithm," *IEEE Trans. Antennas Propag.*, vol. 62, no. 5, pp. 2736–2744, May 2014.

[3] T. Su, M. Li, and R. Chen, "Domain decomposition scheme with equivalence spheres for the analysis of aircraft arrays in a large-scale range," *Eng. Anal. Boundary Elements*, vol. 73, pp. 42–49, Dec. 2016.

[4] K. Konno, Q. Chen, and R. J. Burkholder, "Numerical analysis of large-scale finite periodic arrays using a macro block-characteristic basis function method," *IEEE Trans. Antennas Propag.*, vol. 65, no. 10, pp. 5348–5355, Oct. 2017.

[5] M. S. Tong, Y. Q. Zhang, R. P. Chen, and C. X. Yang, "Fast solutions of volume integral equations for electromagnetic scattering by large highly anisotropic objects," *IEEE Trans. Microw. Theory Techn.*, vol. 62, no. 7, pp. 1429–1436, Jul. 2014.

[6] B. Zhou and D. Jiao, "Direct finite-element solver of linear complexity for large-scale 3-D electromagnetic analysis and circuit extraction," *IEEE Trans. Microw. Theory Techn.*, vol. 63, no. 10, pp. 3066–3080, Oct. 2015.

[7] S. Hughey, H. M. Aktulga, M. Vikram, M. Lu, B. Shanker, and E. Michielssen, "Parallel wideband MLFMA for analysis of electrically large, nonuniform, multiscale structures," *IEEE Trans. Antennas Propag.*, vol. 67, no. 2, pp. 1094–1107, Feb. 2019.

[8] R. F. Harrington, "Boundary integral formulations for homogeneous material bodies," *J. Electromagn. Waves Appl.*, vol. 3, no. 1, pp. 1–15, Jan. 1989.

[9] A. F. Peterson, S. L. Ray, and R. Mittra, *Computational Methods for Electromagnetics*. New York, NY, USA: IEEE Press, 1998.

[10] W. C. Chew, E. Michielssen, J. Song, and J.-M. Jin, *Fast and Efficient Algorithms in Computational Electromagnetics*. Norwood, MA, USA: Artech House, 2001.

[11] J. M. Jin, *Theory and Computation of Electromagnetic Fields*. Hoboken, NJ, USA: Wiley, 2011.

[12] R. F. Harrington, *Field Computation by Moment Methods*. Piscataway, NJ, USA: IEEE Press, 1993.

[13] L. N. Medgyesi-Mitschang, J. M. Putnam, and M. B. Gedera, "Generalized method of moments for three-dimensional penetrable scatterers," *J. Opt. Soc. Amer. A, Opt. Image Sci.*, vol. 11, no. 4, pp. 1383–1398, Apr. 1994.

[14] S. Rao, D. Wilton, and A. Glisson, "Electromagnetic scattering by surfaces of arbitrary shape," *IEEE Trans. Antennas Propag.*, vol. AP-30, no. 3, pp. 409–418, May 1982.

[15] E. Bleszynski, M. Bleszynski, and T. Jaroszewicz, "AIM: Adaptive integral method for solving large-scale electromagnetic scattering and radiation problems," *Radio Sci.*, vol. 31, no. 5, pp. 1225–1251, Sep./Oct. 1996.

[16] J.-Y. Xie, H.-X. Zhou, W. Hong, W.-D. Li, and G. Hua, "A highly accurate FGG-FG-FFT for the combined field integral equation," *IEEE Trans. Antennas Propag.*, vol. 61, no. 9, pp. 4641–4652, Sep. 2013.

[17] J. R. Phillips and J. K. White, "A precorrected-FFT method for electrostatic analysis of complicated 3-D structures," *IEEE Trans. Comput.-Aided Design Integr. Circuits Syst.*, vol. 16, no. 10, pp. 1059–1072, Oct. 1997.

[18] S. M. Seo and J.-F. Lee, "A single-level low rank IE-QR algorithm for PEC scattering problems using EFIE formulation," *IEEE Trans. Antennas Propag.*, vol. 52, no. 8, pp. 2141–2146, Aug. 2004.

[19] J. M. Tamayo, A. Heldring, and J. M. Rius, "Multilevel adaptive cross approximation (MLACA)," *IEEE Trans. Antennas Propag.*, vol. 59, no. 12, pp. 4600–4608, Dec. 2011.

[20] K. Zhao, M. N. Vouvakis, and J.-F. Lee, "The adaptive cross approximation algorithm for accelerated method of moments computations of EMC problems," *IEEE Trans. Electromagn. Compat.*, vol. 47, no. 4, pp. 763–773, Nov. 2005.

[21] J. Maurin, A. Barka, V. Gobin, and X. Juvigny, "Domain decomposition method using integral equations and adaptive cross approximation IE-ACA-DDM for studying antenna radiation and wave scattering from large metallic platforms," *IEEE Trans. Antennas Propag.*, vol. 63, no. 12, pp. 5698–5708, Dec. 2015.

[22] V. Rokhlin, "Rapid solution of integral equation of scattering theory in two dimensions," *J. Comput. Phys.*, vol. 86, no. 2, pp. 414–439, 2015.

[23] R. Coifman, V. Rokhlin, and S. Wandzura, "The fast multipole method for the wave equation: A pedestrian prescription," *IEEE Antennas Propag. Mag.*, vol. 35, no. 3, pp. 7–12, Jun. 1993.

[24] M. A. Saville, "Multilevel multipole-free fast algorithm for electromagnetic scattering problems in layered media," Univ. Illinois Urbana-Champaign, Champaign, IL, USA, Tech. Rep., 2006.

[25] H. Wallen, S. Jarvenpaa, P. Yla-Oijala, and J. Sarvas, "Broadband Müller-MLFMA for electromagnetic scattering by dielectric objects," *IEEE Trans. Antennas Propag.*, vol. 55, no. 5, pp. 1423–1430, May 2007.

[26] X. Zhao, Z. Lin, Y. Zhang, S.-W. Ting, and T. K. Sarkar, "Parallel hybrid method of HOMoM–MLFMA for analysis of large antenna arrays on an electrically large platform," *IEEE Trans. Antennas Propag.*, vol. 64, no. 12, pp. 5501–5506, Dec. 2016.

[27] Y. Zhang, M. Taylor, T. Sarkar, A. De, M. Yuan, H. Moon, and C. Liang, "Parallel in-core and out-of-core solution of electrically large problems using the RWG basis functions," *IEEE Antennas Propag. Mag.*, vol. 50, no. 5, pp. 84–94, Oct. 2008.

[28] Q. Su, X. Zhao, Z. Gu, Y. Zhang, and T. Mao, "Parallel integral equation based nonoverlapping DDM for solving electrically-large scattering problems in half space," *IEEE Access*, vol. 6, no. 10, pp. 59308–59315, Oct. 2018.

[29] Q. Su, Y. Liu, X. Zhao, Z. Gu, C. Zhai, Z. Lin, and W. Wu, "Parallel integral equation-based nonoverlapping DDM for solving challenging electromagnetic scattering problems of two thousand wavelengths," *Int. J. Antennas Propag.*, vol. 2019, pp. 1–10, Jan. 2019.

[30] Z. Peng, X.-C. Wang, and J.-F. Lee, "Integral equation based domain decomposition method for solving electromagnetic wave scattering from non-penetrable objects," *IEEE Trans. Antennas Propag.*, vol. 59, no. 9, pp. 3328–3338, Sep. 2011.

[31] L.-W. Guo, Y. Chen, J. Hu, R. Zhao, M. Jiang, J. L.-W. Li, and Z. Nie, "A novel JMCFIE-DDM for analysis of EM scattering and radiation by composite objects," *IEEE Antennas Wireless Propag. Lett.*, vol. 16, pp. 389–392, 2017.

[32] Z. Peng, K.-H. Lim, and J.-F. Lee, "Computations of electromagnetic wave scattering from penetrable composite targets using a surface integral equation method with multiple traces," *IEEE Trans. Antennas Propag.*, vol. 61, no. 1, pp. 256–270, Jan. 2013.

[33] W.-D. Li, W. Hong, and H.-X. Zhou, "An IE-ODDM-MLFMA scheme with DILU preconditioner for analysis of electromagnetic scattering from large complex objects," *IEEE Trans. Antennas Propag.*, vol. 56, no. 5, pp. 1368–1380, May 2008.

[34] J. Chen, M. Wang, S. Li, M. Zhu, J. Yu, and X. Li, "An IE-ODDM scheme combined with efficient direct solver for 3D scattering problems," *Microw. Opt. Technol. Lett.*, vol. 55, no. 9, pp. 2027–2033, Sep. 2013.

[35] Y. Liu, Q. Su, X. Zhao, Y. Zhang, Z. Lin, C. Zhai, and Q. Zhang, "Accurate analysis of JEM interference in airborne array using parallel HO-IE-DDM," *Appl. Comput. Electromagn. Soc.*, vol. 34, no. 3, pp. 425–433, Mar. 2019.

[36] O. Wiedenmann and T. F. Eibert, "A domain decomposition method for boundary integral equations using a transmission condition based on the near-zone couplings," *IEEE Trans. Antennas Propag.*, vol. 62, no. 8, pp. 4105–4114, Aug. 2014.

[37] Z. Peng, K.-H. Lim, and J.-F. Lee, "A discontinuous Galerkin surface integral equation method for electromagnetic wave scattering from nonpenetrable targets," *IEEE Trans. Antennas Propag.*, vol. 61, no. 7, pp. 3617–3628, Jul. 2013.

[38] K.-L. Zheng, H.-X. Zhou, and W. Hong, "Integral equation-based nonoverlapping DDM using the explicit boundary condition," *IEEE Trans. Antennas Propag.*, vol. 63, no. 6, pp. 2739–2745, Jun. 2015.

[39] Z. Peng, R. Hiptmair, Y. Shao, and B. MacKie-Mason, "Domain decomposition preconditioning for surface integral equations in solving challenging electromagnetic scattering problems," *IEEE Trans. Antennas Propag.*, vol. 64, no. 1, pp. 210–223, Jan. 2016.

[40] M. S. Tasic and B. M. Kolundzija, "Method of moment weighted domain decomposition method for scattering from large platforms," *IEEE Trans. Antennas Propag.*, vol. 66, no. 7, pp. 3577–3589, Jul. 2018.
[41] S. M. Rao, "A true domain decomposition procedure based on method of moments to handle electrically large bodies," *IEEE Trans. Antennas Propag.*, vol. 60, no. 9, pp. 4233–4238, Sep. 2012.
[42] K. Han, Z. Nie, M. Jiang, Y. Chen, and J. Hu, "A novel implementation of IEDG-based DDM for solving electromagnetic scattering from large and complex PEC objects," *Electromagnetics*, vol. 38, no. 1, pp. 1–19, Jan. 2018.
[43] M. J. Gander, "Schwarz methods over the course of time," *Electron. Trans. Numer. Anal.*, vol. 31, pp. 228–255, 2008.

YING-YU LIU was born in Shaanxi, China, in 1991. She received the B.S. degree in electronic information engineering from Xidian University, in 2013 and 2017, respectively, where she is currently pursuing the Ph.D. degree. Her research interests include the large-scale parallel method of moment computation of electrically large electromagnetic targets, domain decomposition method, and fast multipole method.

MING-DA ZHU (Member, IEEE) received the B.S., M.S., and Ph.D. degrees from Shanghai Jiao Tong University, Shanghai, China, in 2005, 2008, and 2012, respectively.

From 2015 to 2018, he was an Associate Professor with the School of Information Science and Technology, Donghua University, Shanghai. Since October 2017, he has been a Visiting Scholar with the Department of Electrical Engineering and Computer Science, Syracuse University, Syracuse, NY, USA. He is currently an Associate Professor with the School of Electronic Engineering, Xidian University, Xi'an, China. His research interests include computational electromagnetics with focus on frequency- and time-domain integral equations.

CHANG ZHAI was born in Shaanxi, China, in 1992. He received the B.S. degree in intelligence science and technology and the M.S. degree in electronics and communications engineering from Xidian University, Xi'an, China, in 2014 and 2017, respectively, where he is currently pursuing the Ph.D. degree.

His current research interests include computational electromagnetic, domain decomposition method, and antenna optimization.

PENG HOU was born in Shaanxi, China, in 1995. He received the B.S. degree in electronic and information engineering from Xidian University, Xi'an, China, in 2017, where he is currently pursuing the Ph.D. degree.

His current research interests include computational electromagnetic, parallel computing, and electromagnetic scattering.

YU ZHANG received the B.S., M.S., and Ph.D. degrees from Xidian University, Xi'an, China, in 1999, 2002, and 2004, respectively. In 2004, he joined Xidian University as a Faculty Member. He was a Visiting Scholar and an Adjunct Professor with Syracuse University, from 2006 to 2009. As a Principal Investigator, he works on projects, including the Project of NSFC. He has authored four books *Parallel Computation in Electromagnetics* (Xidian University Press, 2006), *Parallel Solution of Integral Equation-Based EM Problems in the Frequency Domain* (Wiley IEEE, 2009), *Time and Frequency Domain Solutions of EM Problems Using Integral Equations and a Hybrid Methodology* (Wiley, 2010), and *Higher Order Basis Based Integral Equation Solver* (Wiley, 2012), as well as more than 100 journal articles and 40 conference papers.